Supplementary Information for

Digital Logic for Soft Devices

Daniel J. Preston, Philipp Rothemund, Haihui Joy Jiang[†], Markus P. Nemitz[†], Jeff Rawson, Zhigang Suo, George M. Whitesides

To whom correspondence may be addressed: George M. Whitesides
Email: gwhitesides@gmwgroup.harvard.edu
[†] Indicates equal contribution.

This PDF file includes:

> Supplementary text
> Figs. S1 to S8
> Caption for Movie S1

Other supplementary materials for this manuscript include the following:

> Movie S1

Supplementary Text

Soft, Pneumatic Logic Gate Fabrication

We used two different commercially-available elastomers manufactured by Smooth-On: Dragon Skin 10NV (semi-transparent) and Smooth-Sil 950 (blue). Their prepolymer mixtures were prepared in three steps: (i) adding the two components, A and B, (ii) mixing the components by manually stirring them, and (iii) degassing the mixture under vacuum. The prepolymer mixture of Dragon Skin 10NV was prepared by mixing its two components in a 1:1 ratio, stirring the mixture manually for ~ 2 min, and degassing for ~ 5 min. The pre-polymer mixture of Smooth-Sil 950 was prepared by mixing its components in a 10:1 ratio, stirring the mixture for ~ 5 min, and degassing for ~ 10 min.

The degassed prepolymer elastomers were filled into 3D-printed molds and cured to create the valve components (input files for the 3D-printer for all molds are uploaded as Data File S1 to the auxiliary supplementary materials). To fabricate the tubing inside the valve, we filled a syringe with the prepolymer mixture of Smooth-Sil 950 and degassed it inside the syringe for an additional 10 min before injecting the contents of the syringe into the assembled mold (Fig. S1) through an opening at the bottom. The conical tip (Dragon Skin 10NV) and the component used to connect the tubing to the conical tip (Smooth-Sil 950) were made with two separate molds (Fig. S1). These two components were fabricated by pouring the pre-polymer mixture into their molds, allowing any air bubbles to rise to the surface and pop, and covering the molds with a microscope cover slip to ensure a homogenous thickness. We cured the pieces for 24 hours at room temperature before demolding. After demolding, the tubes were cut to the desired length (two 11 mm tubes and two 20 mm tubes per valve). We glued the pieces together (Fig. S2) using Dragon Skin 10 NV, and cured the tubing assembly at 60 °C for 10 min.

To fabricate the cylindrical walls, membrane, and flat faces of the valve, we filled molds with prepolymer Dragon Skin 10NV (Fig. S3) and waited until all the air bubbles in the mixture disappeared. For the horizontal channels in the flat faces, we inserted 16-gauge needles into the molds through openings in their sides before filling the molds with the prepolymer mixture of Dragon Skin 10NV. The molds for the flat face were covered with microscope cover slips to ensure a homogenous thickness, while the mold for the combined cylindrical wall-membrane assembly of the devices has a lid, containing ventilation holes, so that excess material is squeezed out when the lid is placed onto the mold. We cured the elastomers in these molds for two hours at room temperature before demolding. After demolding, we cut off the excess material on the cylindrical wall-membrane assembly, present due to the ventilation holes, with scissors.

At each end of the cylindrical wall-membrane assembly, we punched out a hole of 3 mm diameter (~ 5 mm from the end) (Fig. S3) to connect tubing to the inner chambers of the valve.

The tubing was glued into the top flat face (11-mm long, fabricated as above) and bottom flat face (20-mm long) (Fig. S4). We also glued the tip of the bottom tubing onto the bottom of the membrane. Finally, we glued the flat faces to the cylindrical walls of the valve (Fig. S4). For the gluing process, we used Dragon Skin 10NV as glue, and cured the glue after each step for 10 min at 60°.

Experimental Characterization

The soft valve was characterized with the experimental setup shown in Figure S6 to generate the data provided in the main text, Figures 2 and 3. We varied one or two input pressures with voltage-controlled pressure regulators (SMC Pneumatics ITV 0010-2BL) interfaced to a computer, and we characterized and recorded input, output, and supply pressures with electronic pressure sensors (Panasonic ADP5151) connected to a DAQ (NI USB-6218 BNC). The constant supply pressure (binary **1**) was set with a manual pressure regulator (Watts 03904). Input pressures were turned on and off as step functions with a five second delay between transitions.

The same experimental setup was used to control the input pressures and to characterize the input and output pressures for the SR latch, two-bit shift register, and digital-to-analog converter (DAC) presented in the main text, Figures 4-6. In these experiments, the logic circuits were constructed from multiple valves, but, with regard to experimental measurements, were treated as "black boxes," that is, blocks of logic that require a set number of inputs and, based on these inputs, produce a set number of outputs. The DAC required one modification: three constant input pressure levels were needed, so two additional manual pressure regulators (Watts 03904) were used to generate the 50 and 100 mbar sources of pressure.
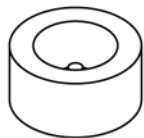
A

16 gauge needles
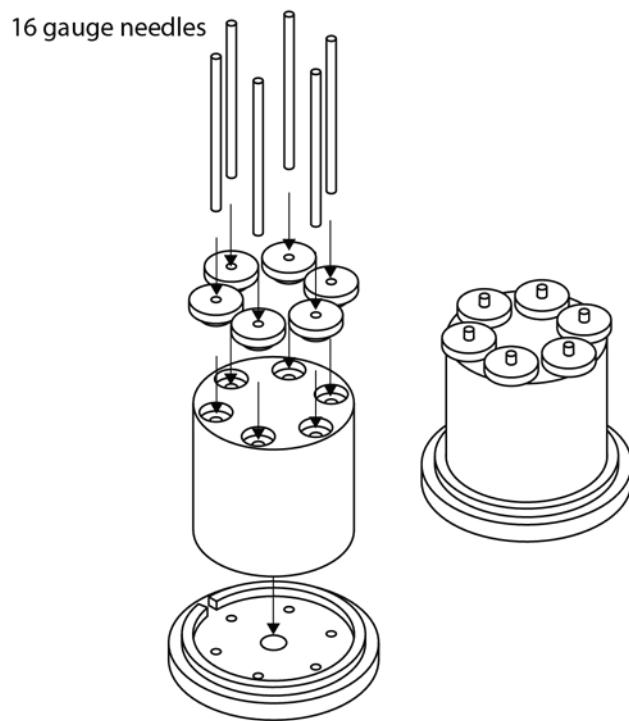
B
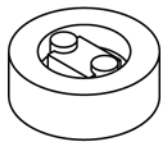
C

Fig. S1. Designs of the molds for the tubing used inside the chambers of the valves. (A) Assembly of the mold to fabricate six tubes, simultaneously. (B) Mold for the connector (between the tubing and the conical tip). (C) Mold for the conical tip.
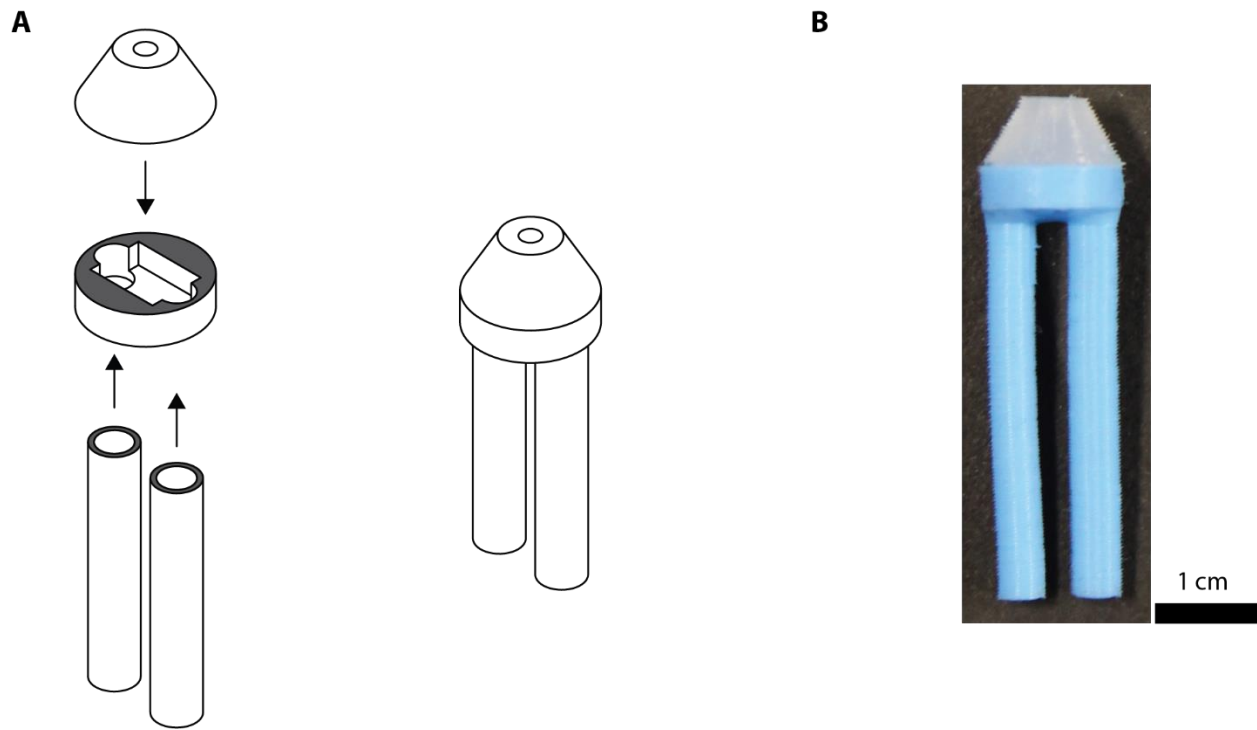
A

B

Fig. S2. Assembly of the tubing used inside the chambers of the valve. (A) The gray areas mark the locations where glue was applied. Alignment of the tubes with the connector is facilitated by keeping syringe needles in the tubes during the assembly. (B) Photograph of the assembled tubing.
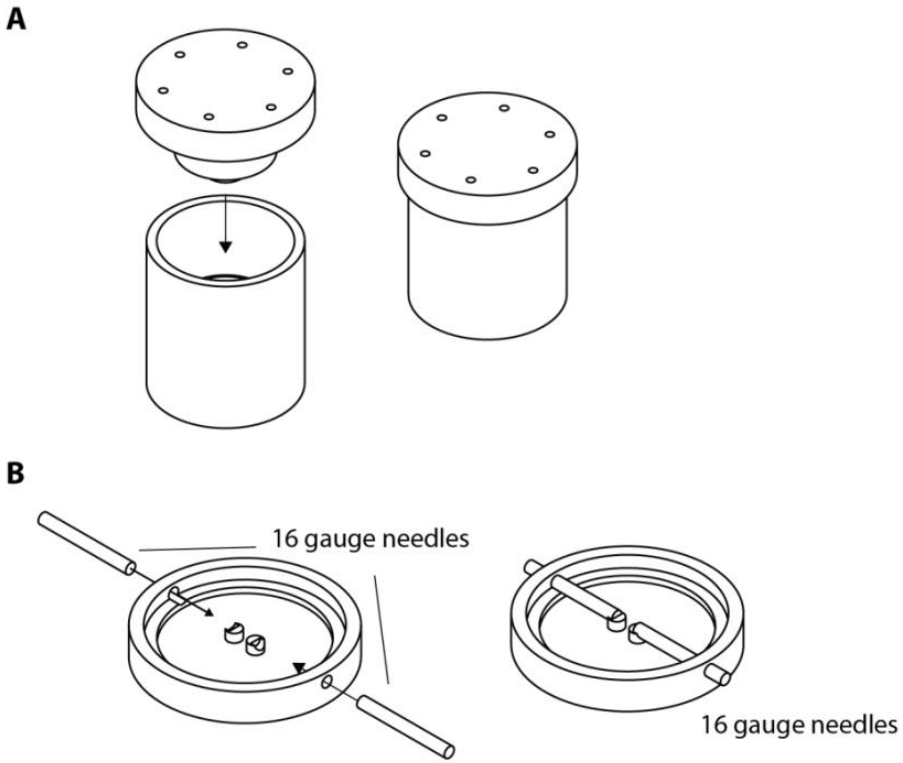
1 cm

A

B

16 gauge needles

16 gauge needles

Fig. S3. Designs of the molds for the valve. (A) Mold for the cylindrical wall-membrane assembly. (C) Mold for the top and bottom flat faces with internal channels for flow of air.
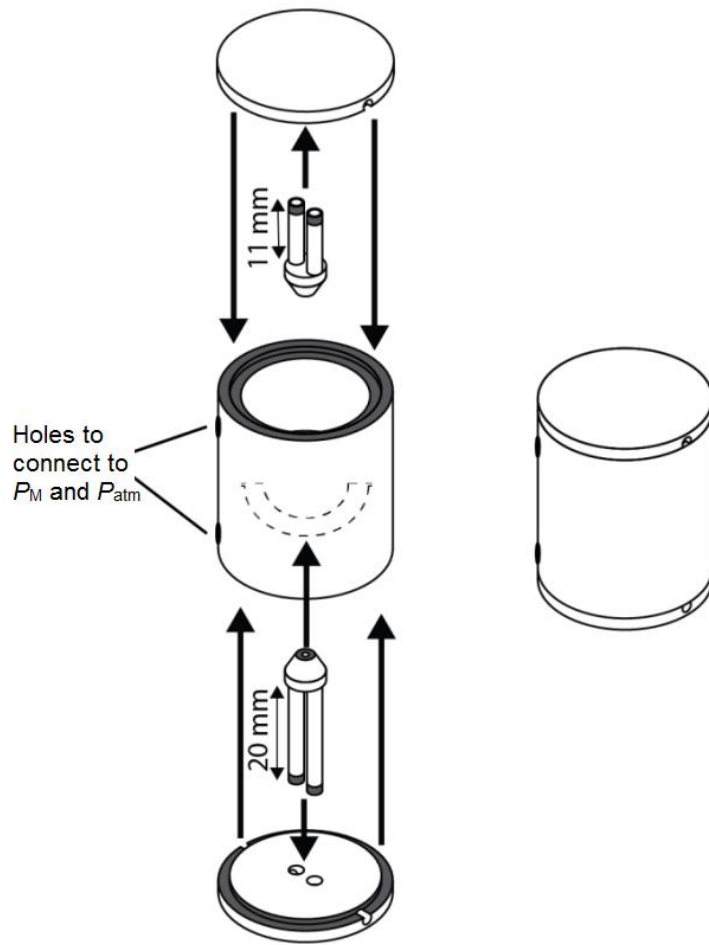
Fig. S4. Assembly of the valve. The gray areas mark locations where adhesive was applied and the elastomeric sections were bonded.
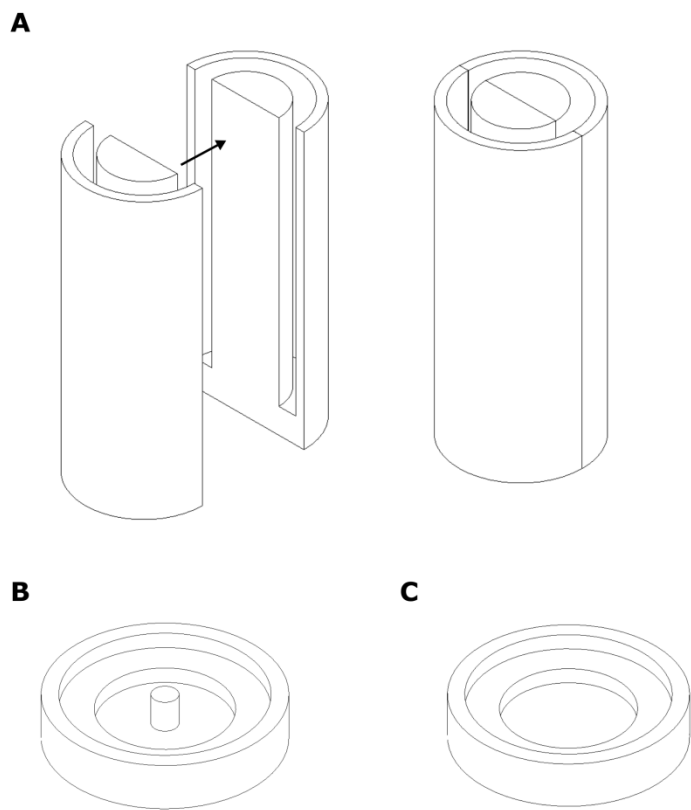
Fig. S5. Molds for the submersible soft robot. The outer shell (A) is composed of two parts that attach to each other. The top (B) and bottom (C) panels are then attached to the outer shell after the digital logic components are inserted.
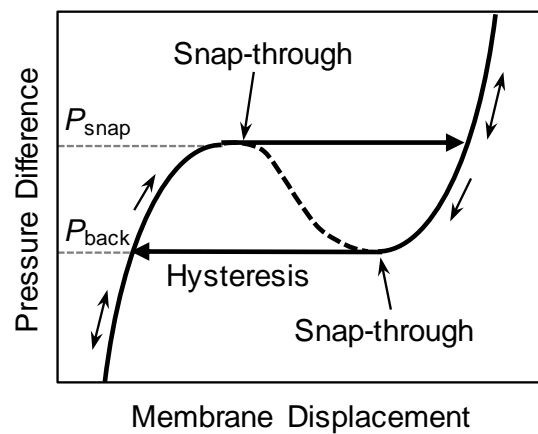
Fig. S6. Membrane snap-through hysteresis is shown here. The membrane snaps downwards at pressure difference P_{snap}, and upwards (to its resting state) at pressure difference P_{back}.

NOT logic gate

A	0	1
Q	1	0

Traditional (TTL, single MOS, etc.) construction

Steady-state energy consumption

CMOS construction
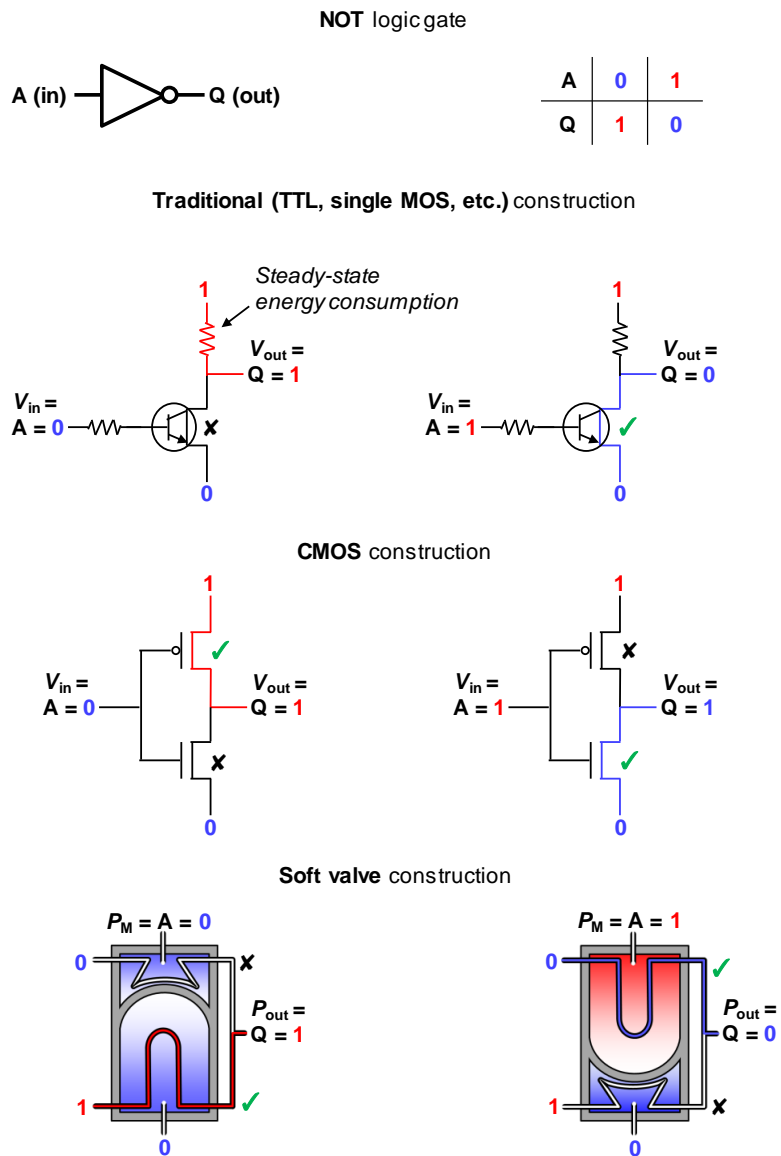
Soft valve construction

Fig. S7. Comparison of electronic digital logic with soft digital logic. A NOT logic gate inverts its input signal (**A**) to an output (**Q**) with the opposite logical value. A traditional electronic NOT gate, using transistor-transistor logic (TTL) or metal-oxide-semiconductor (MOS) with a single doping, consumes energy at steady state. This energy consumption results from the pull-up or pull-down resistors associated with logic gates based on these types of transistors, which are required to specify the output state. Digital logic based on complementary metal-oxide-semiconductor (CMOS) devices, however, allows for switching of two complementary pathways simultaneously, using a single input signal, and therefore precludes the requirement for pull-up or pull-down resistors within the system. The soft NOT gate presented in this work is similar to its CMOS-based counterpart in that, upon actuation (or deactuation) of the NOT gate, one pneumatic pathway is closed, while the other is simultaneously opened.
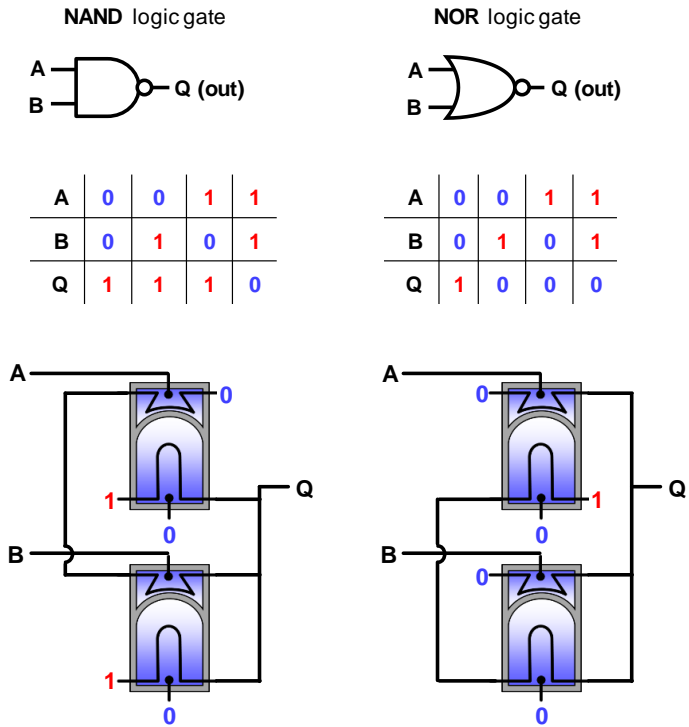
NAND logic gate

NOR logic gate

A	0	0	1	1
B	0	1	0	1
Q	1	1	1	0

A	0	0	1	1
B	0	1	0	1
Q	1	0	0	0

Fig. S8. Schematics detailing the construction of NAND and NOR logic gates. The NAND logic gate outputs **1** in every case except when both of the inputs (**A** and **B**) are **1**. The NOR logic gate outputs 1 only when both of the inputs (**A** and **B**) are **0**. Both of these logic gates require two soft valves each, limiting their applicability in logic circuits that could typically be simplified by implementation of NAND and NOR gates (like the D-type latch used in the two-bit shift register).
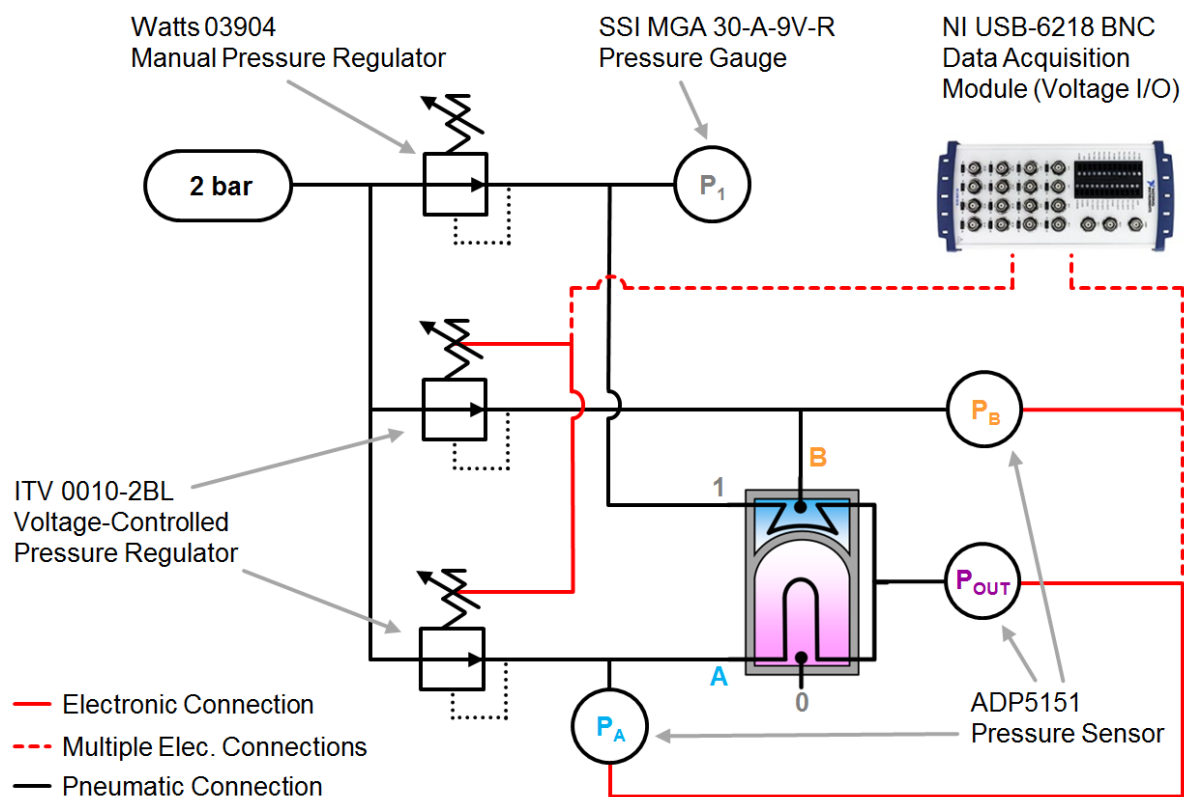
Fig. S9. Experimental setup. Each soft pneumatic logic gate was tested in the above experiment (OR gate configuration shown). We varied input pressures with two voltage-controlled pressure regulators interfaced to a computer. We characterized and recorded input and output pressures with electronic pressure sensors connected to a DAQ.
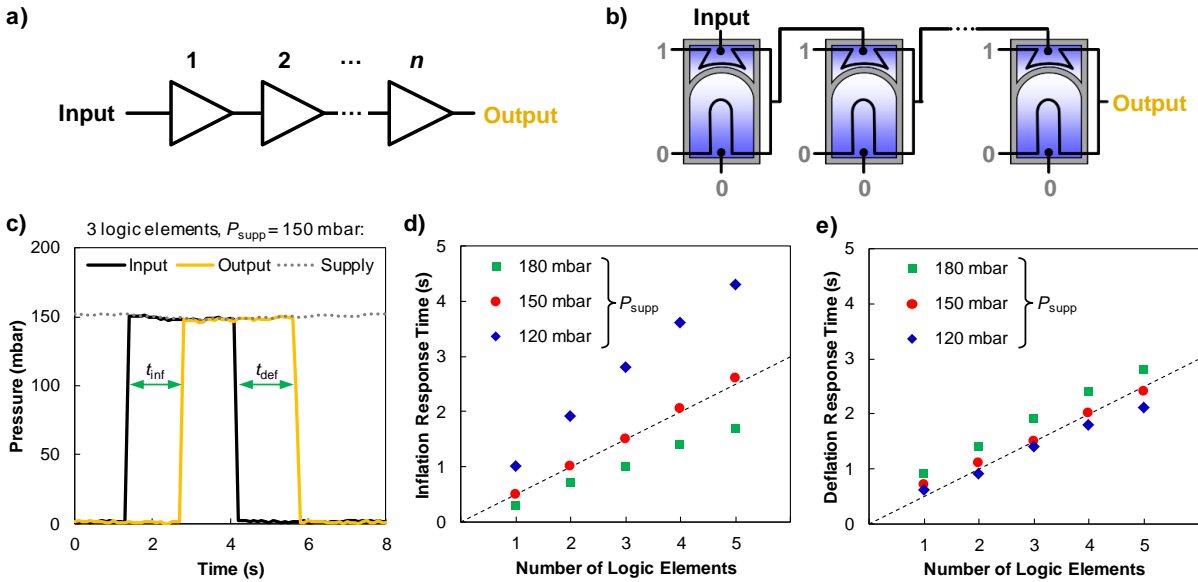
Fig. S10. Logic gate response time during inflation and deflation. We created a chain of followers (buffers) with n total logic elements to characterize the response time of each element (a), configured as shown (b). For a given number of logic elements and supply pressure, P_{supp} (corresponding to binary **1**), we calculated response time during inflation (forward snap-through) of all of the valves, t_{inf}, and during deflation (snap-back), t_{def}, with these quantities described in (c). The characteristic response time during inflation of logic elements was faster at higher supply pressure due to the higher driving force for inflation (d). Conversely, the characteristic response time during deflation of logic elements was slower at higher supply pressure, which can be understood by considering that more pressurized air must be driven out during deflation from a higher starting pressure. The black dashed curve represents a response time of 0.5 sec per logic element; at a supply pressure of 150 mbar, both the inflation and deflation characteristic response times are approximately 0.5 sec per element over any number of logic elements.
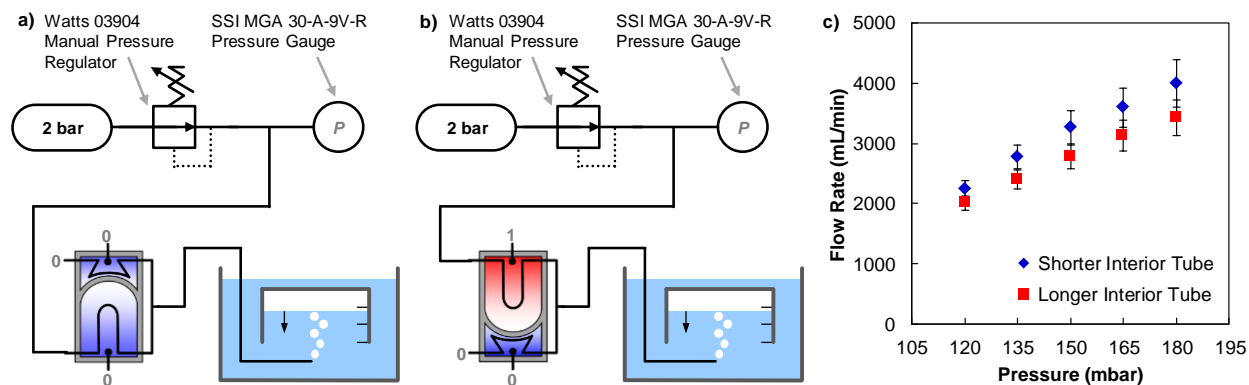
Fig. S11. Volumetric flow rate through the soft digital logic elements. The flow rate was characterized through both the shorter section of interior tubing (a), and through the longer interior tubing (b). Pressurized air, with pressure controlled by a regulator and recorded with an electronic pressure gauge, was forced through the interior tubing of the logic element, then collected in an inverted container of known volume (300 mL) inside of a larger, upright reservoir of water. The hydrostatic pressure at the bottom of the water-filled reservoir was less than 10 mbar, and therefore did not introduce significant error. Experimentally-measured flow rates varied from 2,000 to 4,000 mL/min as a function of pressure at the inlet, but did not vary by more than 15% from the shorter to the longer lengths of inner tubing.
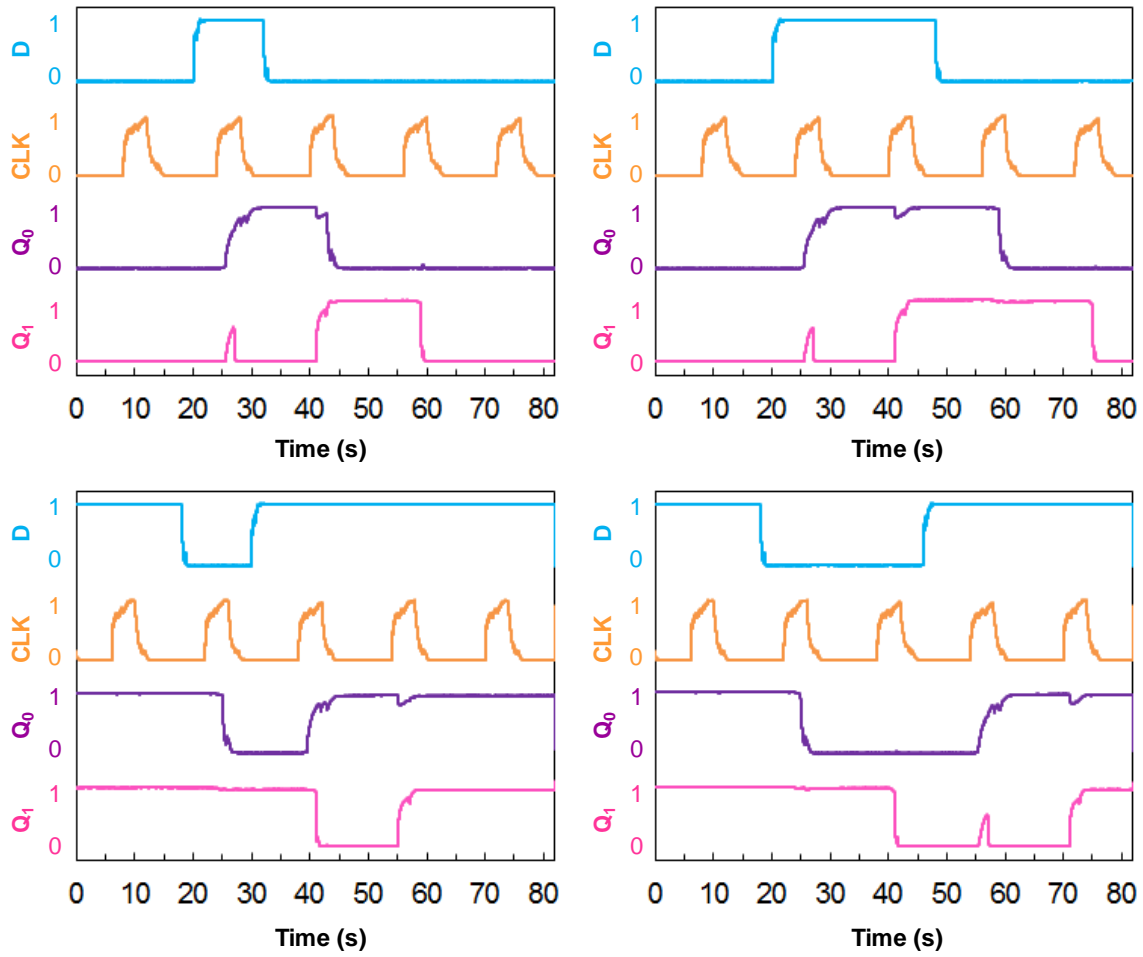
Fig. S12. Shift register data, characterized with the experimental setup detailed in Figure S6, for various input (D) signals with the same periodic clock (CLK) signal.
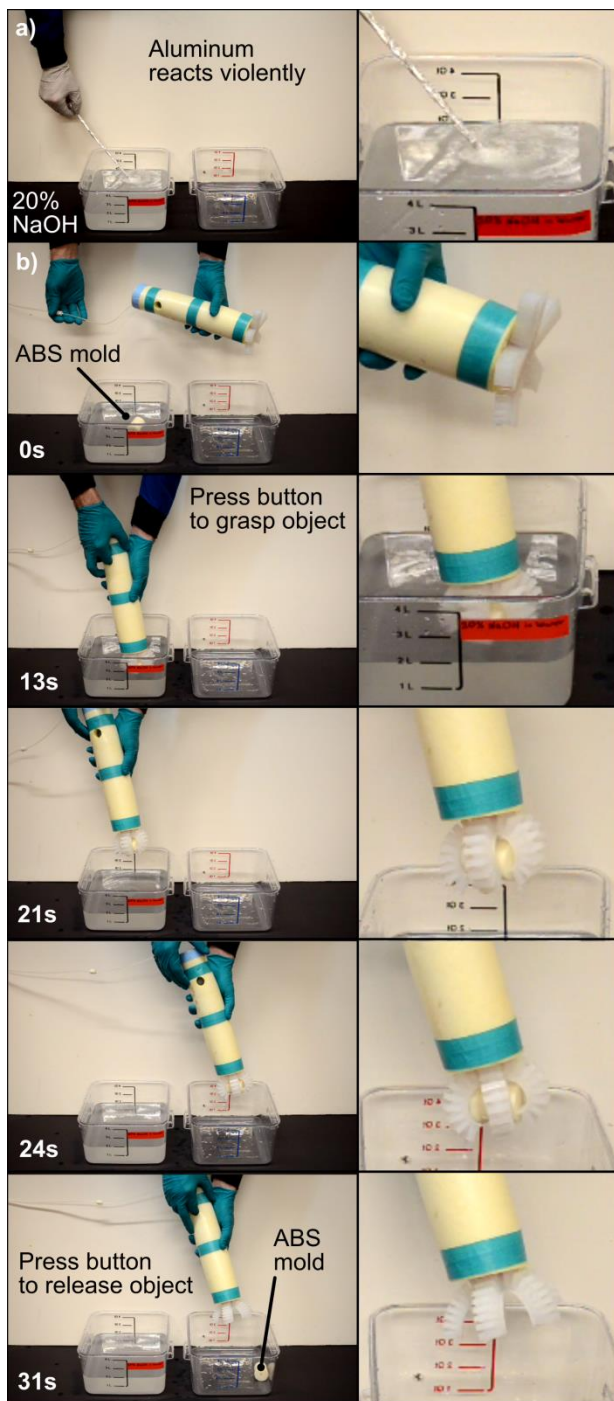
Fig. S13. Human-operated, completely soft gripper with toggle button. We demonstrated the chemical resistance of the soft gripper in a base bath of 20% sodium hydroxide (by weight) in water, strong enough to cause a metal (aluminum) to react and degrade within seconds (a). A 3D-printed ABS mold was placed in the base bath to remove support material introduced by the 3D printer; a human user retrieved the mold from the base bath by pressing the single soft button to toggle between the actuated and unactuated states of the pneu-net gripper ((b); see Supplementary Movie S1).

Movie S1. The soft gripper with toggle button grasping an object. We demonstrated the chemical resistance of the soft gripper in a base bath of 20% sodium hydroxide (by weight) in water, which caused a metal (aluminum) to react and degrade within seconds. A 3D-printed ABS mold was placed in the base bath to remove support material introduced by the 3D printer; a human user then retrieved the mold from the base bath by pressing the single soft button to toggle between the actuated and unactuated states of the pneu-net gripper.

Movie S2. The submersible soft robot. This robot autonomously and repeatedly dives and surfaces over a period of approximately 1 minute, enabling applications where continuous underwater sampling is required without hard components, for example, to avoid detection, or to handle delicate samples. The robot can be summoned to the surface at any time by a human user upon the press of a soft button.